Progress in Photovoltaics: Research and Applications

AN INVESTIGATION INTO HOT-SPOTS IN TWO LARGE GRID-CONNECTED PV PLANTS

Journal:	*Progress in Photovoltaics: Research and Applications*
Manuscript ID:	PIP-08-013.R1
Wiley - Manuscript type:	Applications
Date Submitted by the Author:	n/a
Complete List of Authors:	Muñoz, Javier; Universidad Politécnica de Madrid, Instituto de Energía Solar; Universidad Politécnica de Madrid, Electrónica, Automática e Informática Industrial Lorenzo, Eduardo; Universidad Politécnica de Madrid, Instituto de Energía Solar Martínez-Moreno, Francisco; Universidad Politécnica de Madrid, Instituto de Energía Solar Marroyo, Luis; Universidad Pública de Navarra, Ingeniería Eléctrica y Electrónica García, Miguel; Universidad Pública de Navarra, Ingeniería Eléctrica y Electrónica
Keywords:	hot-spot, grid-connection, azimuthal one-axis tracking

AN INVESTIGATION INTO HOT-SPOTS IN TWO LARGE GRID-CONNECTED PV PLANTS

J. Muñoz[(1)], E. Lorenzo[(1)], F. Martínez-Moreno[(1)], L. Marroyo[(2)], M. García[(2)].

[(1)]Instituto de Energía Solar. Universidad Politécnica de Madrid (IES-UPM). Ciudad Universitaria s/n. 28040 Madrid, Spain.

[(2)]Departamento de Ingeniería Eléctrica y Electrónica. Universidad Pública de Navarra. Campus de Arrosadia. 31006 Pamplona, Spain.

Correspondence to:

Javier Muñoz Cano.

Address: Departamento de Electrónica, Automática e Informática Industrial.

Escuela Universitaria de Ingeniería Técnica Industrial. Universidad Politécnica de Madrid.

Ronda de Valencia, 3. 28012 Madrid.

E-mail: javier@ies-def.upm.es

SUMMARY

This paper details an investigation into the appearance of hot-spots in two large grid-connected PV plants, which were detected after the visual inspection of trackers whose energy output was decreasing at anomalous rate. Detected hot-spots appeared not only in the solar cells but also in resistive solder bonds between cells and contact ribbons. Both types cause similar irreversible damage to the PV modules, but the latter are the main responsible for the detected decrease in energy output, which was confirmed in an experimental testing campaign. The results of this investigation, for example: how hot-spots were detected or their impact on the output power of PV modules, may be of interest for the routine maintenance of large grid-connected PV plants.

Keywords: Hot-spot, grid-connection, azimuthal one-axis tracking.

1. INTRODUCTION

A hot-spot has been a well-know phenomenon in photovoltaics (PV) since the early space applications[1]. It defines a localized region in a PV module whose operating temperature is very high in comparison with its surroundings. This can occur when a cell generates less current than the rest of cells connected in series as a result of partial shading, cell damage, mismatching or interconnection failure. As result, the defective cell is reverse-biased and behaves like a load that dissipates the power generated by the rest of cells in the form of heat.

The protection against hot-spots is also well-know and consists of connecting a bypass diode, with reverse polarity, in parallel with a group of cells, typically 12 or 18 for crystalline silicon modules (the term "group" or "group of cells" refer, in this paper, to the cells protected by the same bypass diode). Thus, the defective cell is reverse-biased to a point that causes the forward conduction of the bypass diode, which almost short-circuits the group of cells and ensures that, in the worst case, the aforementioned cell dissipates nearly the power generated by the remaining cells in the group.

Hot-spots suppose a potential risk of irreversible damage for PV modules. They can cause, for example, tedlar delamination, glass breakage, loss of electrical insulation, or even fire. In order to ensure that the PV modules are protected against this damage, international standards[2-5] require that modules must be subjected to hot-spot endurance tests[6,7] before their qualification.

Nevertheless, despite a PV module having the usual qualification certificates, problems can arise in the final deployed modules[8,9] and that those concerning hot-spots are not an exception, as will be shown below. The causes of these field problems may have diverse origins. For example, qualification tests may not be designed for detecting

some subtle failures or because of the manufacturing process. For example, reverse I-V characteristics of solar cells exhibit a large scattering[6,10-12], an information not generally provided by the manufacturers, which makes the prediction of module performance difficult under, for example, partial shading.

This paper details an investigation into the appearance of hot-spots in two large grid-connected PV plants installed in Spain whose names are omitted for reasons of confidence. The only characteristics that concern us are that they are made up of several hundreds of azimuthal one-axis trackers (each one with a nominal power of around 6 kWp and its own energy meter) whose PV modules have 72 cells connected in series and six bypass diodes.

Besides, there are two models of PV modules, hereafter called X and Y, whose crystalline solar cells, nominal power and manufacturer are the same. The model is important because only the X model, which accounts for 65% of the total installed power, is affected by an unusual type of hot-spot that appears in resistive solder bonds (hereafter referred as RSB) between cells and contact ribbons, which has a great impact not only on the degradation of PV modules but also on their energy output. Despite the term hot-spot commonly refers to the type of hot-spot that appear in solar cells, we have maintained here the term for both types calling “RSB hot-spot” to the former and “hot-spot in cell” to the latter.

Hot-spots in cells, which have taken the main discussion of this introduction, have been also detected in both PV plants and contribute to the degradation of PV modules. Nevertheless, this type of hot-spot has received less attention in this paper because it has a low impact on the decrease of the energy output of the PV modules, whose study was

the main objective of the work. Despite of this, we will speculate about their origin and we will mention some observations that may be of interest.

2. BACKGROUND TO THE WORK

The origin of the investigation presented in this paper was a study carried out between December 2004 and December 2006 that compared the energy production of the trackers installed in the plants, which revealed an anomalous decrease in the energy output. For example, figure 1 sets out the mean monthly energy production of two families of trackers with regard to a third family taken as reference. It can be seen that the relative annual decrease in energy production is around 2% for family 1 and 1% for family 2, which is higher than the absolute typical degradation (0·5% per year) of silicon PV modules[13].

Figure 1. Relative mean-monthly energy production of three families of tracker.

Family 1 was made up of trackers that had PV modules of model X, which have visible RSB hot-spots to the naked eye (see figure 2). These hot-spots started to appear between the spring and summer of 2005, in the first operating year of the plants, and seemed to be correlated with the relative decrease in energy production shown in figure 1. This supposed correlation was later confirmed within the framework of an experimental testing campaign whose results are described in the following section.

Figure 2. RSB hot-spots.

Family 2 was made up of trackers whose modules are also model X, but did not show visible hot-spots. Nevertheless, it seemed that there were invisible hot-spots which were also reducing the energy output of the corresponding trackers, although to a lesser extent than family 1. In fact, some of these hot-spots appeared later. For example, between February 2006 and February 2007, 237 modules (around 6% of the X type modules installed in one of the grid connected systems) were detected by visual inspection.

Figure 3 represents the spatial distribution of the previously mentioned 237 modules inside the tracker, which is made up of 36 PV modules (arranged in four strings connected in parallel, each one with 9 modules connected in series). For example, the number 7 located in upper left corner indicates that 7 modules with RSB hot-spots have appeared in this position of the tracker or, in other words, 7 trackers have a module placed in that position that has RSB hot-spots. As conclusion, it can be seen that the appearance of this type of hot-spot is not correlated with the position of the module inside the tracker.

Figure 3. Spatial distribution in the tracker of modules with RSB hot-spots.

In the previous visual inspection, a total of 62 modules with hot-spots in cells were also discovered. This type of hot-spot normally appears in the edges of the upper corners (see figure 4), which is usual in solar cells[6, 10, 14]. The study of this type of hot-spot has not been included in the subsequent testing campaign because it did not seem to be correlated with the observed energy decrease of the trackers.

Figure 4. Hot-spots located in the edges of the upper corners of solar cells.

Nevertheless, it is worth mentioning that hot-spots in cells appear even at low irradiances. When a cell is partially shaded, it must dissipate around the maximum power generated by the remaining cells of its group, which is nearly proportional to the irradiance. In azimuthal one-axis tracking, which is implemented in both grid-connected plants, it is clear that the lower strings receive more shadows during the day than the upper ones, and also that their shadows occur at higher irradiances.

Hence, one could expect that hot-spots should appear preferably in the modules of the lower strings of the tracker, which is what actually happens as the figure 5 illustrates (the meaning of the numbers in this figure is analogous to that of figure 3. For example, the number 11 located in lower left corner of string 1 indicates that 11 trackers have a module placed in that position that has hot-spots in cells). However, although 73% of affected modules are located in strings 1 and 2, it is also true that around a quarter of the hot-spots appeared in modules placed in the strings 3 and 4, which only receive shadows either at the beginning or end of the day when the irradiance is relatively low (<300 $W \cdot m^{-2}$).

Figure 5. Spatial distribution in the tracker of modules with hot-spots in cells.

Finally, family 3, used as reference in figure 1, is made up of trackers that have PV modules of model Y, which accounts for around 35% of the total installed power in both plants. The energy production of these trackers was the expected and their modules did not show RSB hot-spots. Despite this type of hot-spot appearing in model X but not

in model Y, we do not have enough information to explain this correlation. Apart from the visual observations and measurements described in the following section, we have neither carried out a comprehensive analysis of the affected modules nor additional information on the manufacturing process, which may be at the root of the problem. The only external difference between both models is that the collecting buses and solders of model Y seem to have been manufactured using a careful production process (see figure 6).

Figure 6. Details of PV module models X (a) and Y (b).

3. EXPERIMENTAL OBSERVATIONS

3.1 Testing campaign

In order to confirm the observed correlation between RSB hot-spots and the decrease rate of energy production shown in figure 1, an experimental testing campaign was carried out on six trackers of family 1, three of each PV plant. Table 1 summarises the measured maximum power of these trackers extrapolated to Standard Test Conditions (P_{STC}) and its variation (ΔP) regarding the nominal power specified by the manufacturer (P_{NOM}). In the worst case, the power losses are nearly 15%.

Taking into account that trackers without RSB hot-spots have values of P_{STC} from -3% to -5% less than P_{NOM}, the maximum power losses attributable to hot-spots reach around 10-12%. Table 1 also shows that there is a good correlation between the AC energy delivered to the grid, E_{AC}, to the measured power, P_{STC}, for each tracker. In other

words, the ratio of energy production to the measured power (E_{AC}/ P_{STC}) is similar in all of the trackers installed at the same location.

Table 1. Measured power of trackers affected by RSB hot-spots and ratio of AC energy delivered to this power.

After testing the trackers, the I-V characteristics of each individual string and modules with RSB hot-spots were also measured. For example, table 2 shows the P_{STC} of the four strings that belong to tracker A-2. The large variation in string 2 (ΔP=-14·7%) is mainly caused by three modules that have RSB hot-spots. Figure 7 details the measured I-V characteristics of two of these modules (one of them has a single RSB and the other has two RSB located in different groups of cells), which are compared with a module that does not have RSB. It can be observed that each RSB reduces the open-circuit of the module around 7V, which coincides with the voltage of a group of 12 cells (the modules have 72 cells in series and six bypass diodes, i.e., 12 cells per group). In terms of power, each RSB reduces the power generated by the affected group to zero, which accounts for 1/6 of the maximum power of the module.

Table 2. Measured power of the four strings in tracker A-2.

Figure 7. Measured I-V characteristics of three PV modules of string 2 (tracker A-2) extrapolated to STC.

The increase of series resistance in RSB is reported in the literature as a common degradation mechanism of field-aged PV modules[15, 16]. Nevertheless, in our case, the modules are new and the failure occurred within few years, which seems to indicate a specific and faulty manufacturing process. This series resistance is responsible for the irreversible degradation of the affected PV modules, as the following section shows, as well as a part of the measured power losses. Let us illustrate the qualitative impact on the latter with an exercise of simulation.

Imagine a PV module made up of 24 series cells and two bypass diodes that has a RSB whose resistance is R (this module is a third of the real module and it has been chosen for simplicity). This hypothetical module can be represented by the electric scheme of figure 8, where I_D and I_R refer to the current through the upper bypass diode and the resistor R, and V and I refer to the voltage and current of this PV module.

Figure 8. Module made up of 24-series cells with a RSB whose resistance is R.

Assuming that the cells are identical and that they have negligible parasitic series and shunt resistances, figure 9 shows the computer simulation of I-V, I_D-V, and I_C-V characteristics, which have been normalised to the short-circuit current (I_{SC}) and the open-circuit voltage (V_{OC}) of the module. These characteristics are plotted as a function of the parameter r, which is defined as the ratio of R to the characteristic resistance, R_{CH}, of the group of cells protected by the bypass diode. Finally, R_{CH} is defined as the ratio of the open-circuit voltage to the short-circuit current of the group of cells. Hence, in our example, $r=R/R_{CH}=2RI_{SC}/V_{OC}$.

Figure 9. Computer simulation of current-voltage characteristics as a function of r.

Concerning I-V characteristics, it can be observed that as r increases the current and, therefore, the maximum power of the module, P_M, decrease. Figure 10 shows the ratio of P_M as a function of r, $P_M(r)$, to the maximum power of the module for r=0, $P_M(0)$. For large values of r (r>1), this ratio drops to around 0·45, which is lower than 0·5 (the half of the maximum power of the module) owing to the power losses in the upper bypass diode. Observing the I_D-V characteristics, this diode is ON for large values of r, which keeps the upper group of cells and R near short-circuit.

Finally, I_R-V characteristics show the current that passes through R, which reaches its maximum values in the left side of these characteristics. Figure 10 also shows the ratio of the maximum power dissipated in R as a function of r, $P_R(r)$, to the maximum power of the group attainable for r=0, i.e., $P_M(0)/2$. The maximum value of this ratio is around 1 at r≈1, a case in which the bypass diode is ON. Hence, in this case R dissipates around the maximum power of the group of cells (the power dissipation is slightly higher than this value because the voltage across the diode in forward conduction is not zero). As conclusion, a RSB inside a group of cells may reduce the power generated by that group to zero.

Figure 10. Ratios $P_M(r)/ P_M(0)$ and $P_R(r)/[P_M(0)/2]$ as a function of r.

In order to determine the order the magnitude of the RSB, we measured the voltage of some affected modules in open-circuit, V_{OC}, and after connecting a resistive load, V_L (see figure 11). Both measurements allow to calculate the series resistance of

the module, R_S, using the expression $R_S=R_L[(V_{OC}/V_L)-1]$, where R_L is the resistance of the load.

Figure 11. Test for determining the order of magnitude of the RSB.

For example, for the module whose I-V characteristic is displayed in figure **7** for RSB=2, we obtained a value of R_S=52kΩ (V_{OC}≈38V, V_L≈25V, R_L=100kΩ). Assuming that the parasitic series resistance of the solar cells is negligible, the mean resistance per RSB is 26kΩ. As result of this high resistance, the I-V characteristic of this module is similar to the simulated I-V characteristic displayed in figure 9 for r=100.

This type of I-V characteristic is easily detected using a capacitive load because the capacitor voltage reaches a voltage lower than the open-circuit voltage of the module. Nevertheless, as the size of the PV array increases, the detection of RSB through the inspection of the I-V characteristic becomes more and more difficult because the measured V_{OC} may be similar to the expected value.

For example, if a high RSB develops in a group of cells, as the module has six bypass diodes, the measured V_{OC} of the module with a capacitive load would be around 5/6 of the expected value, which would be suspicious. In contrast, if we measure the I-V curve of one string composed of 9 modules connected in series (or 54 groups of cells) with a single RSB, the measured V_{OC} would be around 53/54 of the expected value. This is only a difference of -1·85%, which is usually lower than the uncertainty of the measurements. It is worth mentioning that RSB cannot be detected by measuring the open-circuit voltage with a voltmeter because its input impedance is usually several

orders of magnitude higher than the resistance of the RSB and the measurement would be right.

In summary, although the measurements of the open-circuit voltage and the I-V curve are recommended for the routine maintenance of PV plants[17], they are not reliable indicators for detecting the presence of hot-spots, which advise the use of alternative testing methods. For example, portable infrared cameras are currently available on the market at a relatively low cost (from around 5,000) and provide a suitable diagnostic tool[18] for detecting hot-spots in RSB or in cells as well as identifying bypass diodes that are passing current even if the cells that they protect are fully illuminated.

3.2 Module degradation

As well as the energy losses, RSB may also cause irreversible damage to the modules. In the worst case, they must dissipate the power generated by a group of cells, which can reach several tens of watts, and this dissipation of heat can cause elevated hot-spot temperatures. For example, figure 12 shows an infrared thermal image of a RSB whose temperature is greater than 175ºC, which is higher than the critical temperature of commercial encapsulants[6].

Figure 12. Infrared thermal image of a RSB hot-spot.

Figure 13 shows, although the picture does not do it justice, an extreme case of an incandescent RSB hot-spot. Finally, figure 14 shows some illustrative examples of the damage caused by RSB hot-spots. From left to right, perforation of the tedlar, glass breakage, and evidence of fire in a junction box.

Figure 13. Incandescent RSB hot-spot.

Figure 14. Examples of irreversible damage caused by RSB hot-spots.

4. CONCLUSIONS

An investigation into hot-spots has been presented in this paper with the aim of drawing conclusions that can be of interest for the routine maintenance of large grid-connected PV plants. Hot-spots were detected after the inspection of several trackers whose energy output was decreasing at an anomalous rate.

Hot-spots appear not only in the cells but also in high resistive solder bonds that interconnect cells and contact ribbons. Both types cause similar irreversible damage to the PV modules, but the latter is the main responsible for the detected decrease in energy output.

Hot-spots in cells are less numerous and appeared in around 1% of the total PV modules. Of these, about a quarter are located at the top of the trackers, which only receive shadows when the irradiance is relatively low (<300 $W \cdot m^{-2}$).

Hot-spots in resistive solder bonds appeared in around 4% of the total PV modules. The impact of this type of hot-spot in the output power of PV modules is very important because a single hot-spot may reduce to zero the power generated by a group of cells protected by the same bypass diode.

Finally, it is worth stressing that the detection of hot-spots is very difficult just by observing the I-V characteristic of a PV array and even more so by measuring its open-circuit voltage, which advises the use of infrared imaging equipment for this purpose.

REFERENCES

1. F.A. Blake, K.L. Hanson. The hot-spot failure mode for solar arrays. *Proceedings of the 4th Intersociety Energy Conversion Engineering Conference*. 1969: 575–581.
2. IEC Standard 61215. *Crystalline Silicon Terrestrial Photovoltaic (PV) Modules – Design Qualification and Type Approval*. International Electrotechnical Commission. 1995.
3. IEC Standard 61646. *Thin-Film Terrestrial Photovoltaic (PV) Modules – Design Qualification and Type Approval.* International Electrotechnical Commission. 1997.
4. UL Standard 1703. *UL Standard for Safety for Flat-plate Photovoltaic Modules and Panels*. Underwriters Laboratories. 1993.
5. IEEE Standard 1262-1995. *IEEE Recommended Practice for Qualification of Photovoltaic (PV) Modules*. Institute of Electrical and Electronics Engineers. 1995.
6. Herrmann W., Wiesner W., Vaassen, W. Hot spot investigations on PV modules-new concepts for a test standard and consequences for module design with respect to bypass diodes. *26th IEEE Photovoltaic Specialists Conference*. 1997: 1129–1132.
7. Wohlgemuth J., Herrmann W. Hot spot tests for crystalline silicon modules. *31th IEEE Photovoltaic Specialists Conference*. 2005: 1062-1063.
8. A. Schlumberger. Rebellion of farmers. *Photon International*. September 2006: 54-57.
9. A. Schlumberger. The behemoth awakens – at least, a little. *Photon International*. October 2006: 74-77.
10. Danner M., Bucher K. Reverse characteristics of commercial silicon solar cells-impact on hot spot temperatures and module integrity. *26th IEEE Photovoltaic Specialists Conference*. 1997: 1137–1140.

11. W. Herrmann, M. Adrian, W. Wiesner. Operational behaviour of commercial solar cells under reverse biased conditions. *2nd World Conference on Photovoltaic Solar Energy Conversion*. 1998: 2357–2359.

12. M.C. Alonso-García, J.M. Ruiz, F. Chenlo. Experimental study of mismatch and shading effects in the I–V characteristic of a photovoltaic module. *Solar Energy Materials & Solar Cells*. 2006; **90**: 329–340.

13. C.R. Osterwald, J. Adelstein, J.A. del Cueto, B. Kroposki, D. Trudell, and T. Moriarty. Comparison of degradation rates of individual modules held at maximum power. *4th IEEE World Conference on Photovoltaic Energy Conversion*. 2006; **2**: 2085 – 2088.

14. M. C. Alonso García, W. Herrmann, W. Böhmer, B. Proisy. Thermal and electrical effects caused by outdoor hot-spot testing in associations of photovoltaic cells *Progress in Photovoltaics: Research and Applications*. 2003; **11**: 293-307.

15. D.L. King, M.A. Quintana, J.A. Kratochvil. DE. Ellibee, B.R. Hansen. Photovoltaic Module Performance and Durability Following Long-Term Field Exposure. *Progress in Photovoltaics Research and Applications*. 2000; **8**: 241-256.

16. M. A. Quintana, D. L. King, T. J. McMahon, C. R. Osterwald. Commonly observed degradation in field-aged photovoltaic modules. *29th IEEE Photovoltaic Specialists Conference*. 2002: 1436 – 1439.

17. Kimber A., Mitchell L. Performance evaluation standards for large grid-connected PV systems in the United States and Germany. *20th European Solar Energy Conference*. 2005: 3229-3232.

18. D. L. King, J. A. Kratochvil, and M. A. Quintana, T. J. McMahon. Applications for infrared imaging equipment in photovoltaic cell, module, and system testing. *28th IEEE Photovoltaic Specialists Conference*. 2000: 1487 – 1490.

LIST OF FIGURES

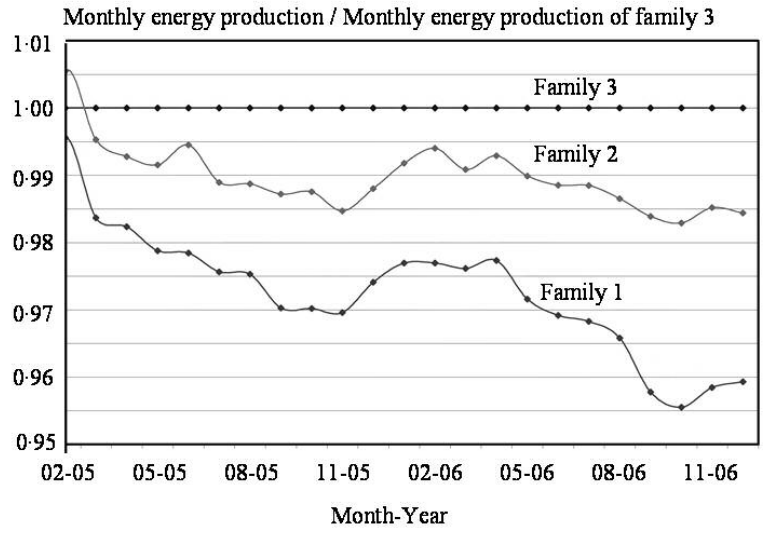

Figure 1. Relative mean-monthly energy production of three families of tracker.

Figure 2. RSB hot-spots.

7	3	8	6	8	4	3	5	6	*String 4*
7	10	11	13	5	9	3	6	5	*String 3*
5	5	5	9	6	8	5	9	9	*String 2*
8	9	6	3	5	8	5	10	3	*String 1*

Figure 3. Spatial distribution in the tracker of modules with RSB hot-spots.

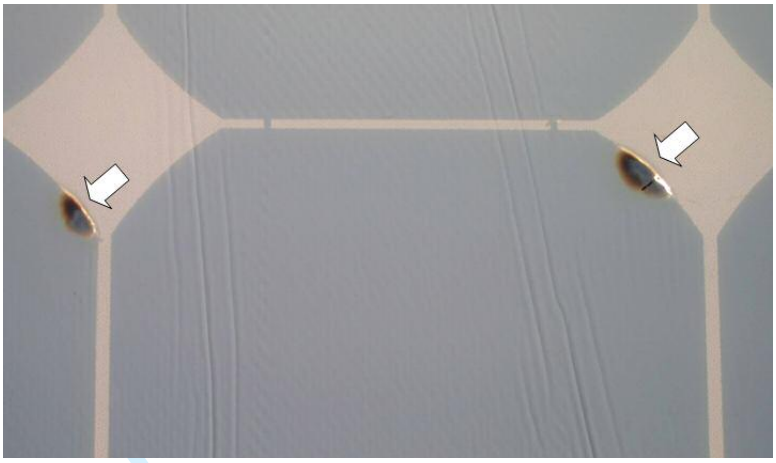

Figure 4. Hot-spots located in the edges of the upper corners of solar cells.

							1		*String 4*
4	6	1	1		1	1	1	1	*String 3*
3	2	2	1		1		2	6	*String 2*
11	6	2				1	2	6	*String 1*

Figure 5. Spatial distribution in the tracker of modules with hot-spots in cells.

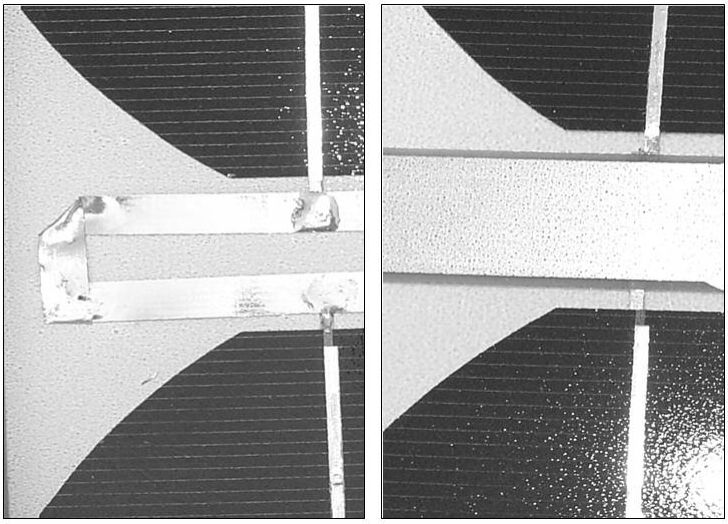

(a) (b)

Figure 6. Details of PV module models X (a) and Y (b).

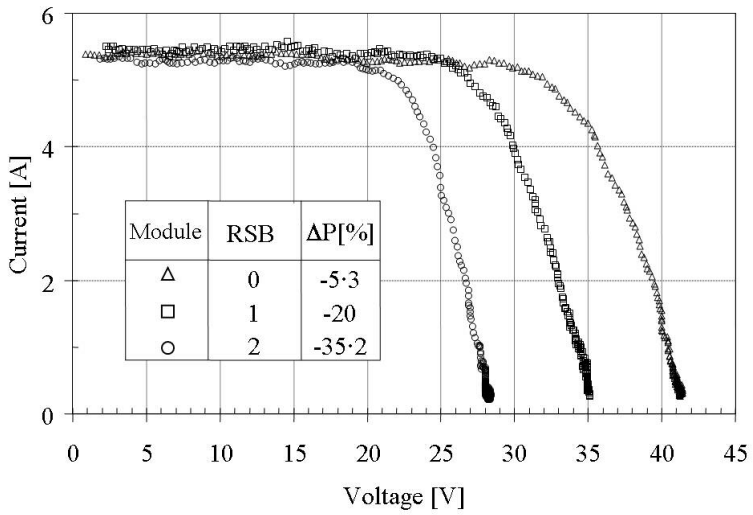

Figure 7. Measured I-V characteristics of three PV modules of string 2 (tracker A-2) extrapolated to STC.

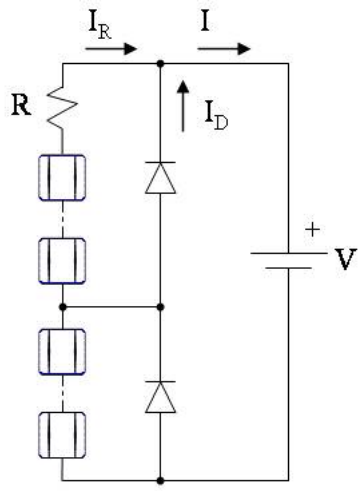

Figure 8. Module made up of 24-series cells with a RSB whose resistance is R.

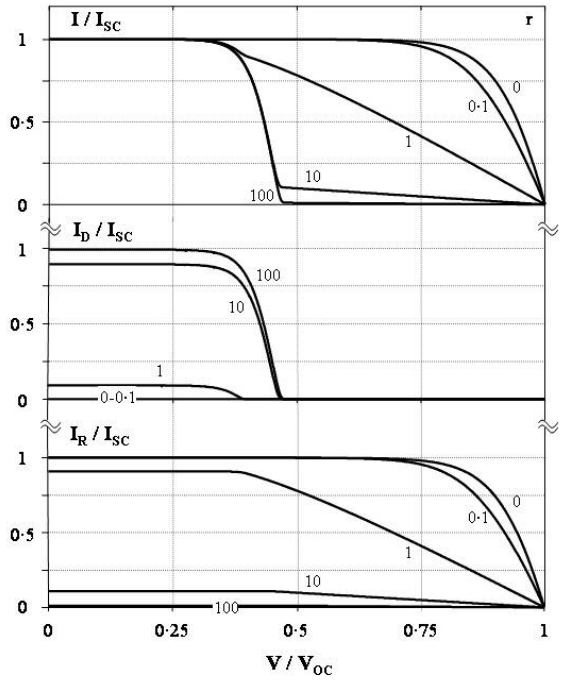

Figure 9. Computer simulation of current-voltage characteristics as a function of r.

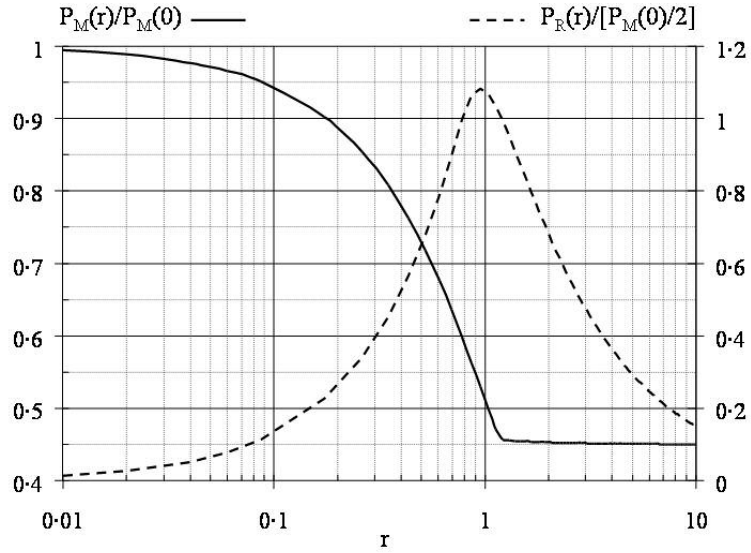

Figure 10. Ratios PM(r)/ PM(0) and PR(r)/[PM(0)/2] as a function of r.

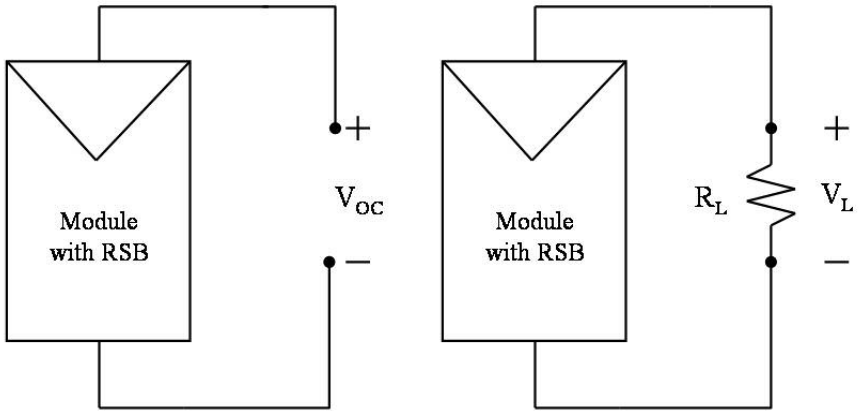

Figure 11. Test for determining the order of magnitude of the RSB.

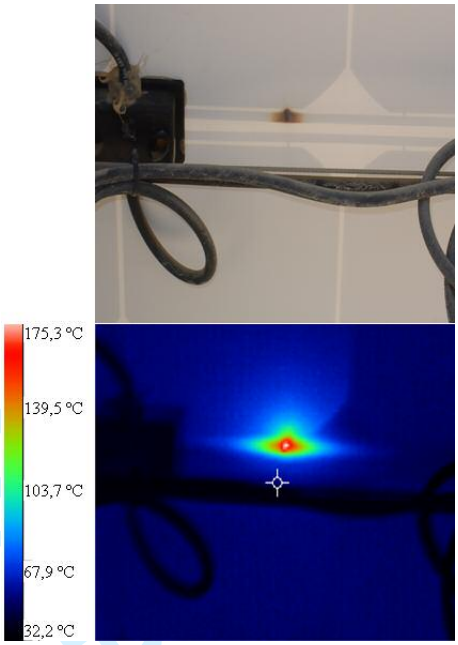

Figure 12. Infrared thermal image of a RSB hot-spot.

Figure 13. Incandescent RSB hot-spot.

Figure 14. Examples of irreversible damage caused by RSB hot-spots.

LIST OF TABLES

Tracker[(*)]	**P_{STC} [W]**	$\Delta P = \frac{P_{STC} - P_{NOM}}{P_{NOM}}$ **[%]**	**E_{AC} [kWh] (Dec 04 – Nov 05)**	**E_{AC}/ P_{STC} [kWh/kW]**
A-1	5647	-7·7	11019	1951
A-2	5209	-14·9	10445	2005
A-3	5344	-12·7	10447	1955
B-1	5526	-9·7	10129	1833
B-2	5299	-13·4	9617	1815
B-3	5226	-14·6	9558	1829

[(*)]Letters A and B indicate a different PV plant.

Table 1. Measured power of trackers affected by RSB hot-spots and ratio of AC energy delivered to this power.

Tracker	String	$\Delta P = \frac{P_{STC} - P_{NOM}}{P_{NOM}}$ [%]
A-2	1 (bottom)	-5·4
	2	-14·7
	3	-3·6
	4 (top)	-3·4

Table 2. Measured power of the four strings in tracker A-2.

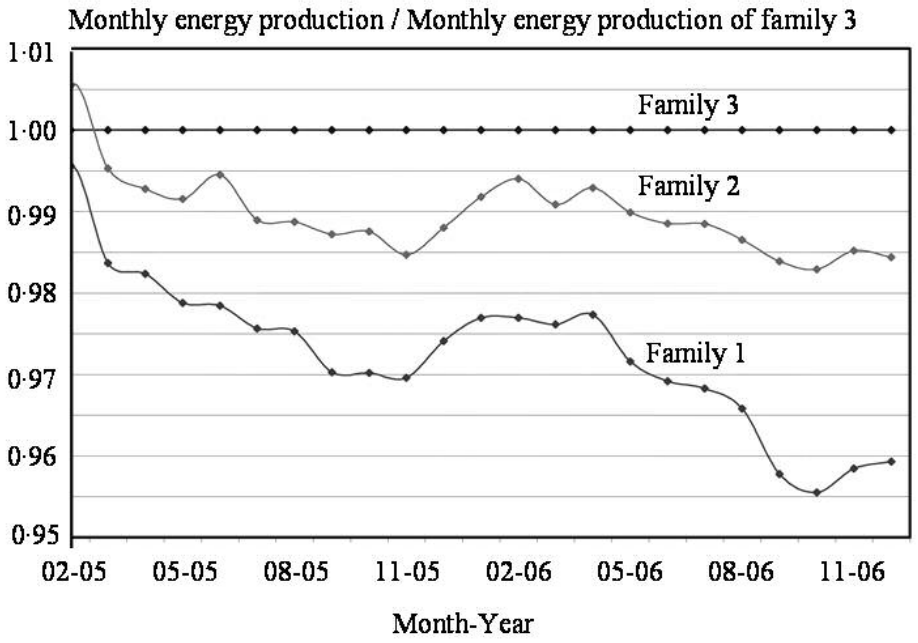

269x190mm (72 x 72 DPI)

200x149mm (72 x 72 DPI)

7	3	8	6	8	4	3	5	6	*String 4*
7	10	11	13	5	9	3	6	5	*String 3*
5	5	5	9	6	8	5	9	9	*String 2*
8	9	6	3	5	8	5	10	3	*String 1*

254x190mm (72 x 72 DPI)

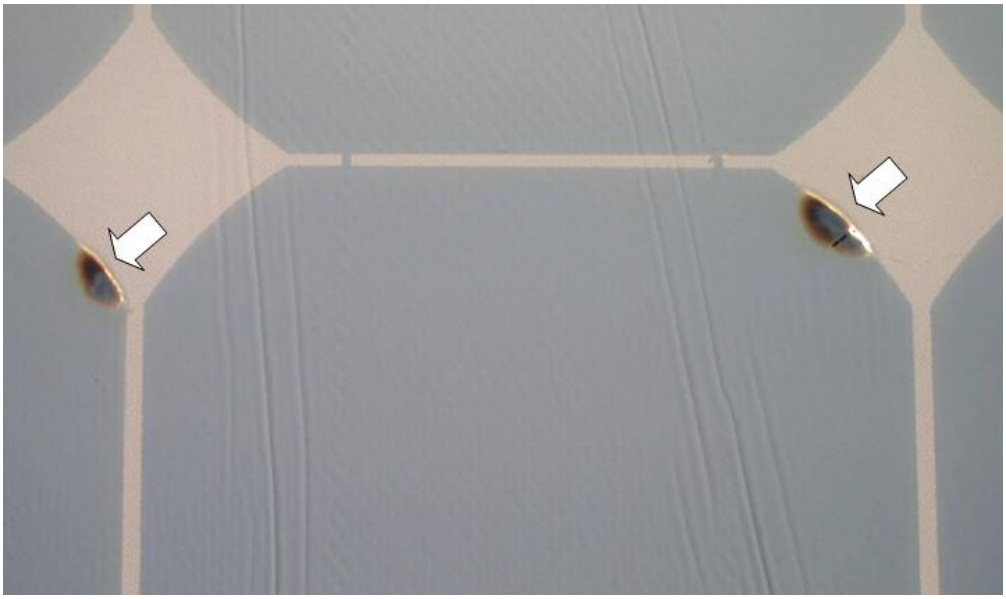

254x149mm (72 x 72 DPI)

							1		*String 4*
4	6	1	1		1	1	1	1	*String 3*
3	2	2	1		1		2	6	*String 2*
11	6	2				1	2	6	*String 1*

254x190mm (72 x 72 DPI)

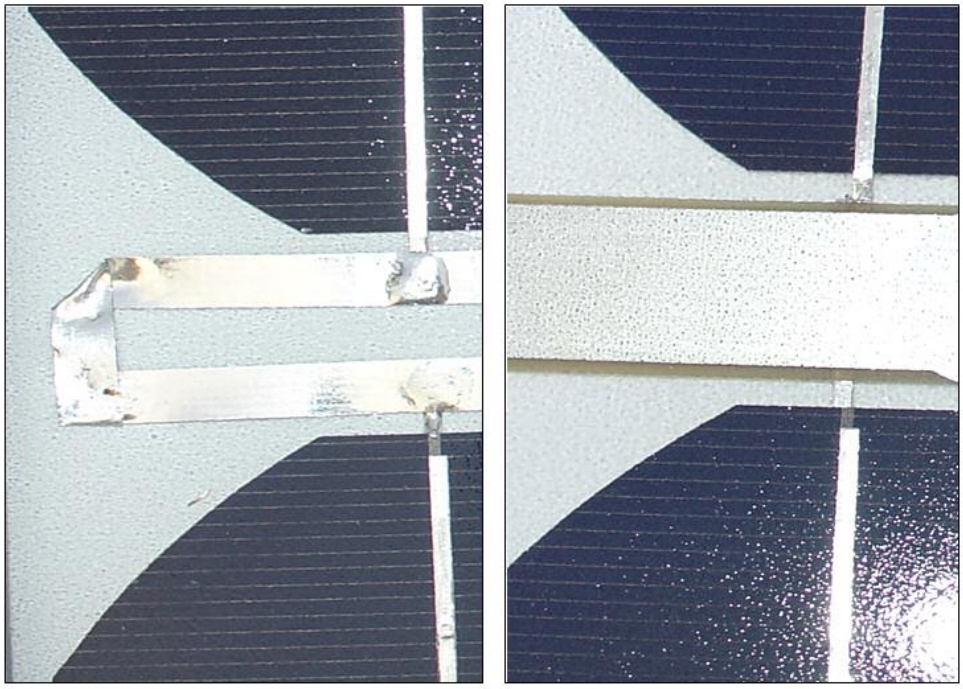

200x139mm (96 x 96 DPI)

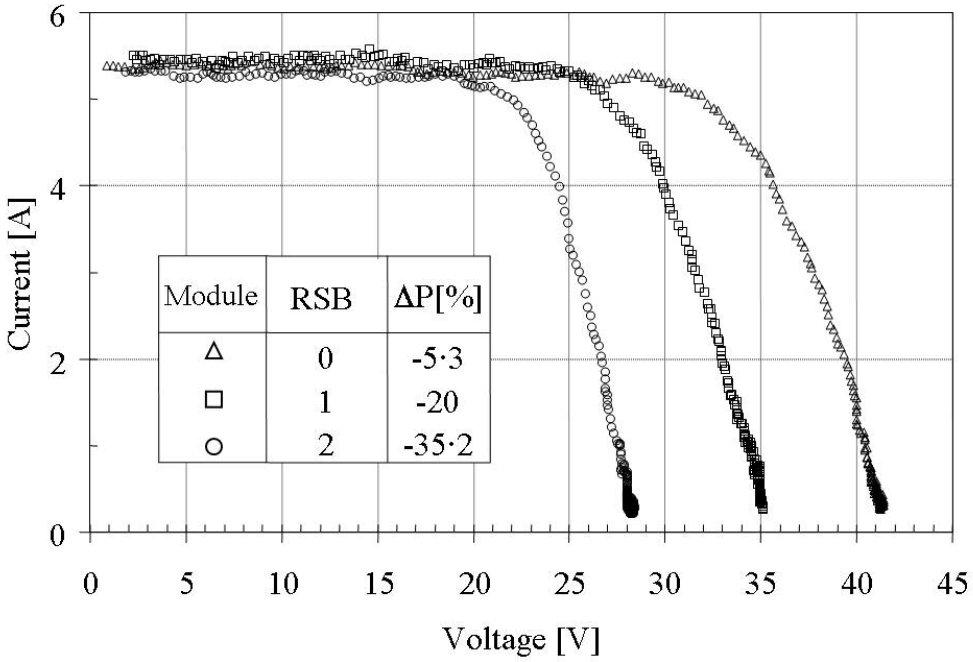

254x190mm (96 x 96 DPI)

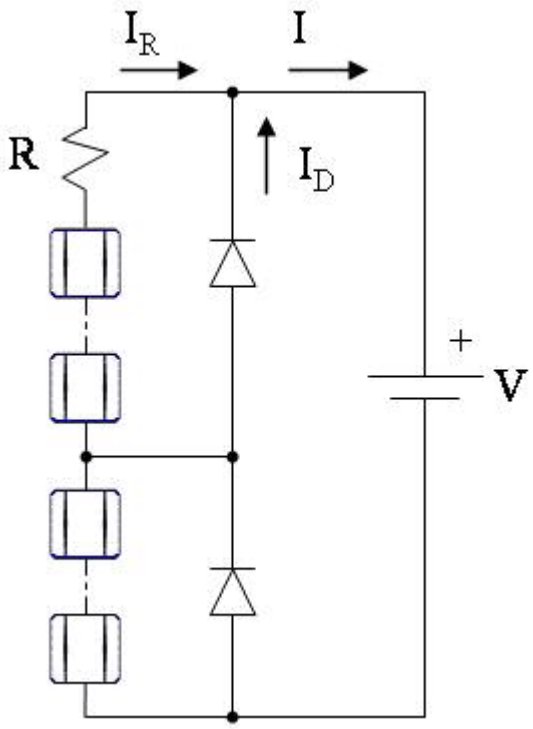

99x129mm (72 x 72 DPI)

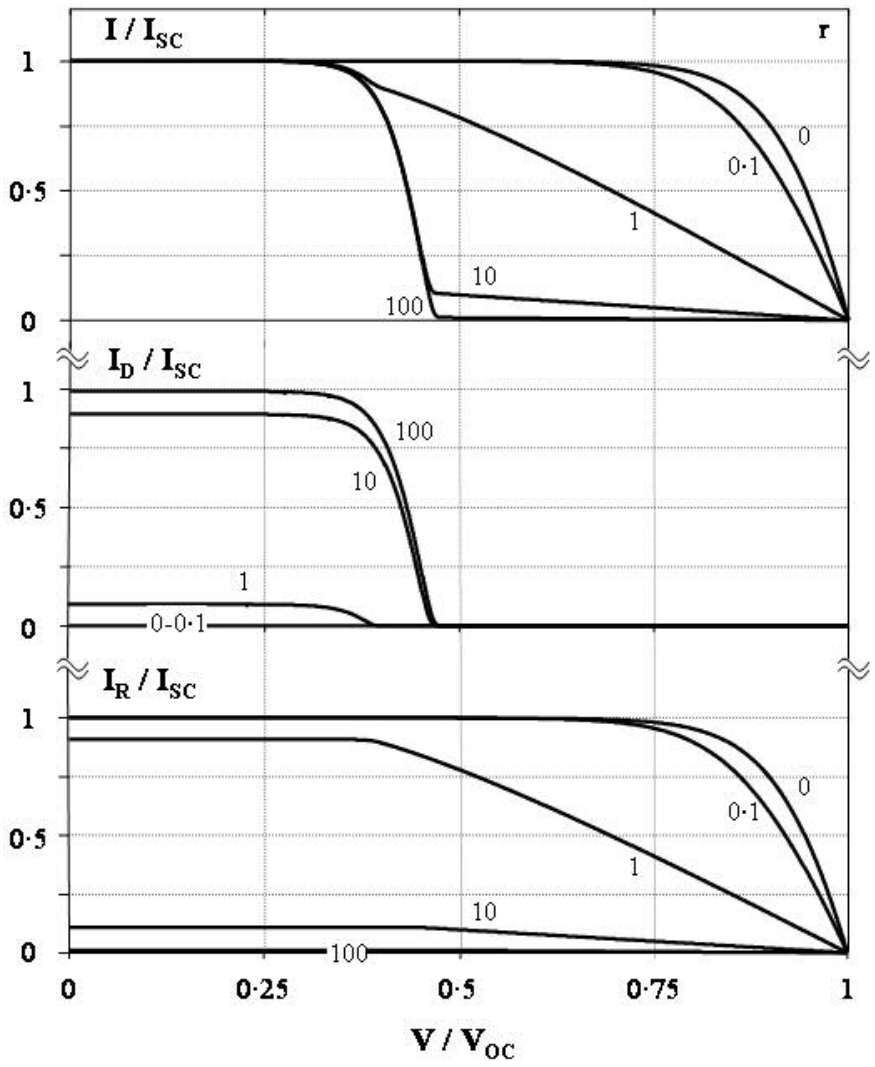

190x254mm (72 x 72 DPI)

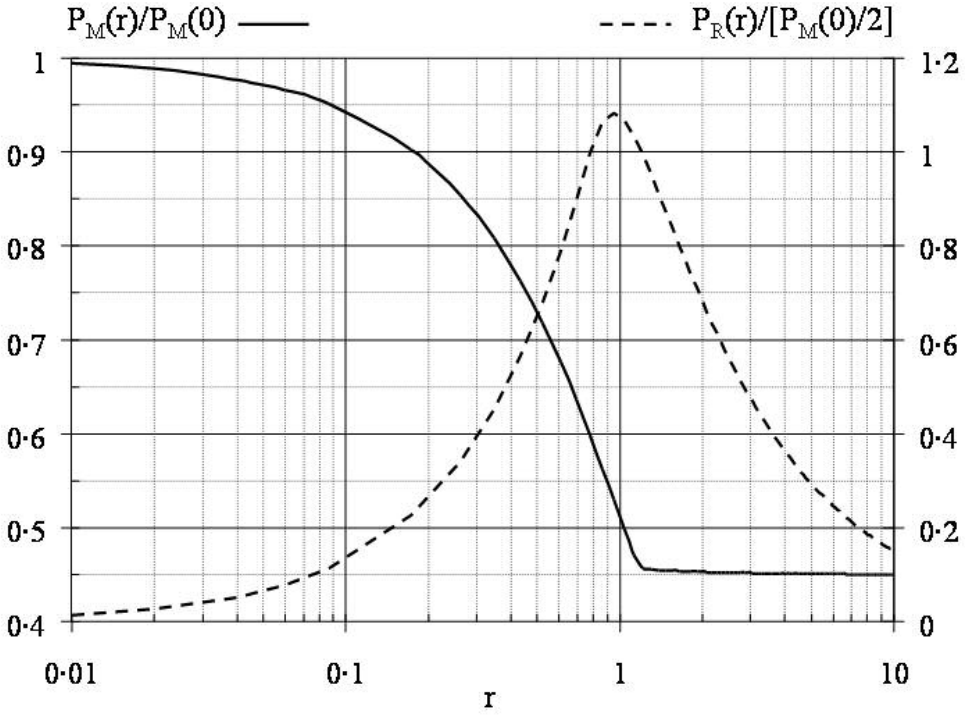

254x190mm (72 x 72 DPI)

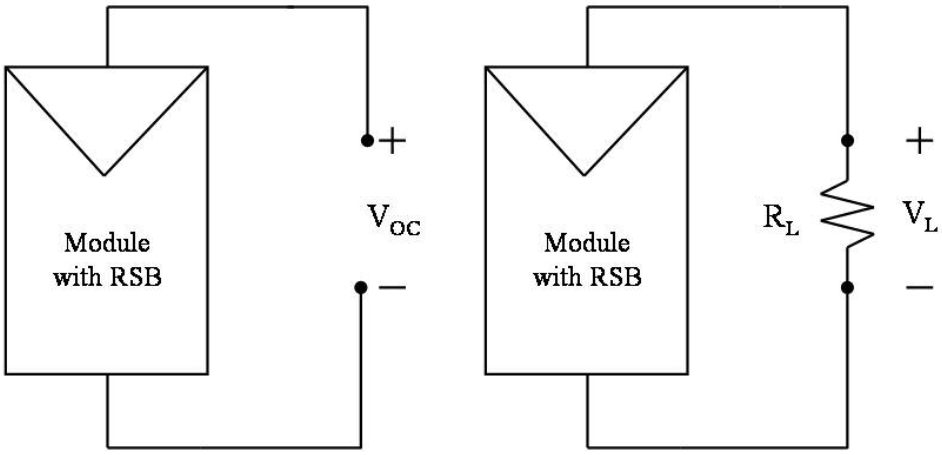

299x149mm (72 x 72 DPI)

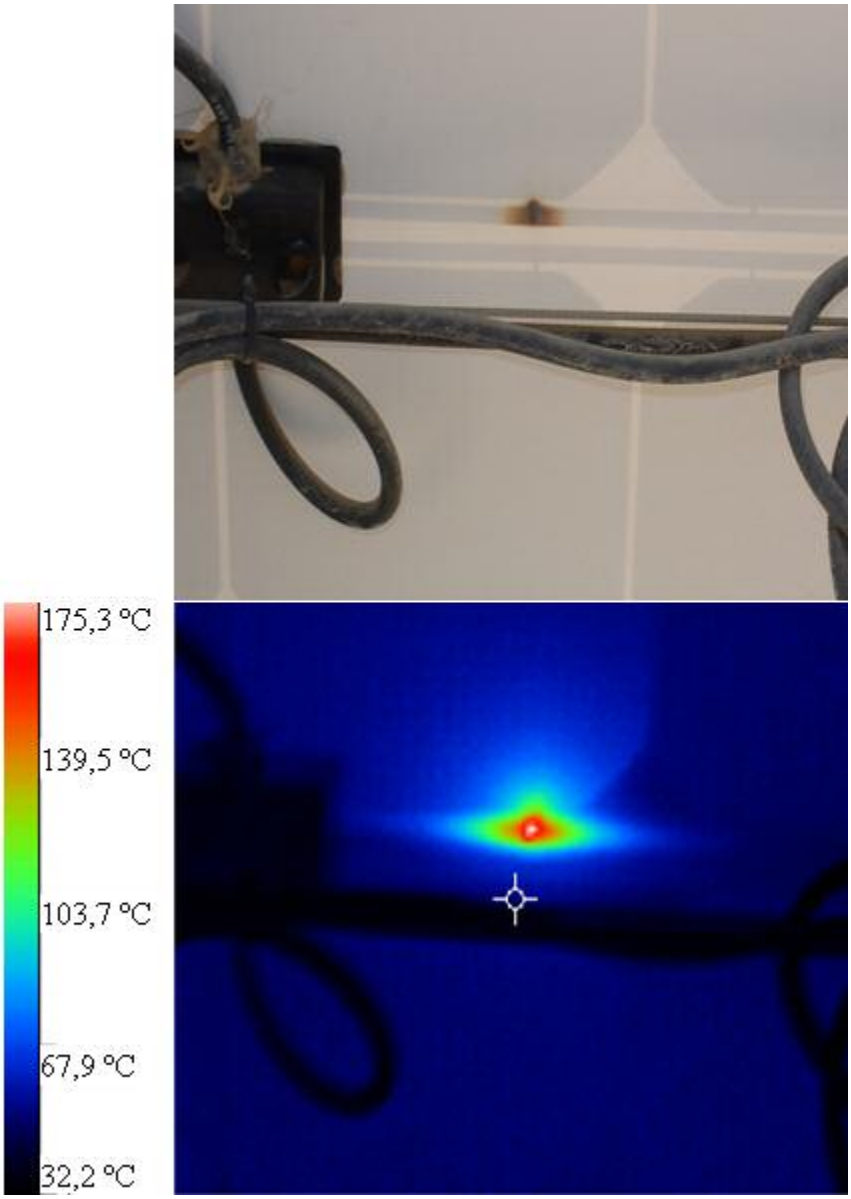

149x209mm (72 x 72 DPI)

79x59mm (72 x 72 DPI)

256x149mm (72 x 72 DPI)